Wan, C., Chen, L., & Cryan, M. J. (2015). Broadband metasurface absorber for solar thermal applications. Journal of Optics, 17(12), 1-7. DOI: 10.1088/2040-8978/17/12/125103

Broadband Metasurface Absorber for Solar Thermal Applications

C.Wan, L.Chen and M.J.Cryan

Department of Electrical and Electronic Engineering, University of Bristol, Bristol, BS8 1UB, UK

Abstract

In this paper we propose a broadband polarization independent selective absorber for solar thermal applications. It is based on a metal-dielectric-metal metasurface structure, but with an inter-layer of absorbing amorphous carbon rather than a low loss dielectric. Optical absorbance results derived from Finite Difference Time Domain modelling are shown for ultra-thin carbon layers in air and on 200nm of gold for a range of carbon thicknesses. A gold-amorphous carbon-gold trilayer with a top layer consisting of a 1D grating is then optimised in 2D to give a sharp transition from strong absorption up to 2μm to strong reflection above 2μm resulting in good solar selective performance. The gold was replaced by the high melting point metal tungsten and is shown to have very similar performance to the gold case. 3D simulations then show that the gold based structure performs well as a square periodic array of squares, however there is low absorption around 400nm. A cross based structure is found to increase this absorption without significantly reducing the performance at longer wavelengths.

Introduction

There has been much work done recently on the use of 2D metamaterials, sometimes termed metasurfaces, as perfect absorbers [1], [2]. This paper explores the use of thin carbon films in metal-dielectric-metal (MDM) structures for solar thermal applications [3]–[5]. Compared with conventional photovoltaic devices, solar thermal converters have the potential to be more efficient since they can use the whole of the solar spectrum [6]. There are also emerging technologies such as solar thermionics [7] and photon-enhanced thermionic emission (PETE) [8] that can benefit from thin, low cost surfaces that can be integrated with materials required for these applications such as lithiated diamond [9]. For solar thermal applications the surface must achieve strong absorption in the visible and near Infrared bands while maintaining high reflectivity in the thermal infrared bands preventing thermal radiation and thus achieving maximum temperature rise [10], [11]. These are known as selective surfaces and have been studied and developed for many years [12]. However, solar thermal technologies increase in efficiency as the upper operating temperature increases and the performance of conventional selective surfaces can degrade at these high operating temperatures, typically ~800 K. Thus this paper aims to use the trilayer MDM structure as a platform for creating broadband selective solar absorbing surfaces that can be integrated into a range of emerging high temperature, solar thermal related technologies.

The MDM trilayer has been widely studied using dielectric material as the absorbing layer in visible spectrum [13], [14], but this paper explores the applications of the structure using a highly absorbing material for solar thermal applications. Solar thermionics is being developed that uses lithiated diamond to create a very efficient electron emitter [9] and if it was possible to integrate the diamond material within a solar absorbing surface this may lead to very low cost technology. Absorbing layers in MDM structures have been studied previously, in [15] a Spin-On-Glass with an absorption resonance in the mid infrared is used to show strong coupling between the metasurface resonance and the absorber. In [16] an MDM structure is incorporated into an organic photovoltaic cell in order to increase solar

absorption. This paper shows the use of a carbon absorbing layer in an MDM structure and the very broadband nature of the carbon absorption could enable many interesting applications. Ideally for solar thermionics a high quality diamond layer would be interesting to explore as the dielectric interlayer. However, this is difficult to achieve currently in practise and thus we focus on amorphous carbon which can be readily deposited in thin layers with controllable thicknesses in the range of 20-50nm. In this paper we will study a particular class of amorphous carbon known as Diamond Like Carbon (DLC) which will be used in future fabrication and measurement studies.

The paper begins with a description of the ideal selective surface required for solar thermal applications. Then the optical properties of DLC are introduced in both bulk and thin film cases. The DLC needs to be placed on a strongly reflecting surface to maintain good infrared reflection and the optical properties of such a structure are then shown. The trilayer structure with a patterned top surface is then introduced and it is shown how this can greatly improve the selectivity of the surface. Optimisation of the structure is then performed to obtain the best selective performance and gold is replaced by the high melting point metal, tungsten which would enable very high temperature operation. Finally a cross type [17] patterned upper layer is introduced which improves the short wavelength absorption while maintaining the longer wavelength performance obtained from a simple square array structure.

Results

Figure 1 shows the simulated solar spectrum modelled as a blackbody at T = 6000K and also the radiated power from an ideal blackbody at 500K, 800K and 1000K [18]. This shows that for solar thermal applications an ideal surface should absorb strongly across the visible range up to 1.5-2μm for applications around 1000K. Above these wavelengths the surface should be strongly reflecting which from Kirchoff's law of thermal radiation will strongly supress thermal infrared emission. Thus we choose a wavelength of 2μm as the transition point between strong absorption and strong reflection.

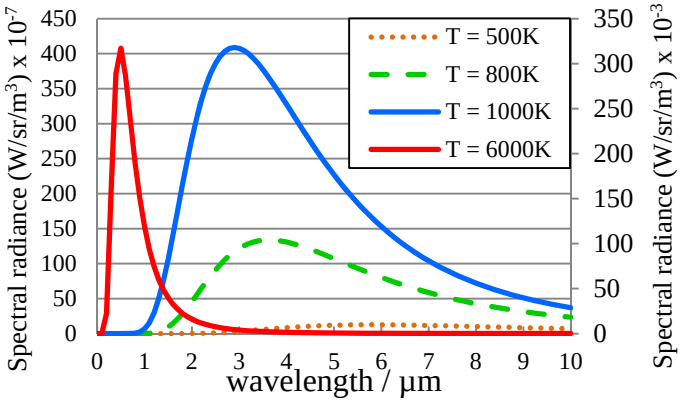

Figure 1: Spectral radiation at T = 500, 800, 1000K (left axis) and 6000K (right axis) vs wavelength, where 6000K case approximates the solar spectrum

DLC is a class of amorphous carbon which contains significant amounts of sp3 hybridized carbon atoms [19]. Amorphous carbon contains a mixture of graphite and diamond clusters that give the material very high optical absorption and wide bandgap [20]. The sublimation point of amorphous carbon is 3915K which will provide enough thermal stability for most solar thermal applications [21]. Figure 2 shows the real and imaginary parts of the refractive index of amorphous carbon from the visible up to 10μm [22].

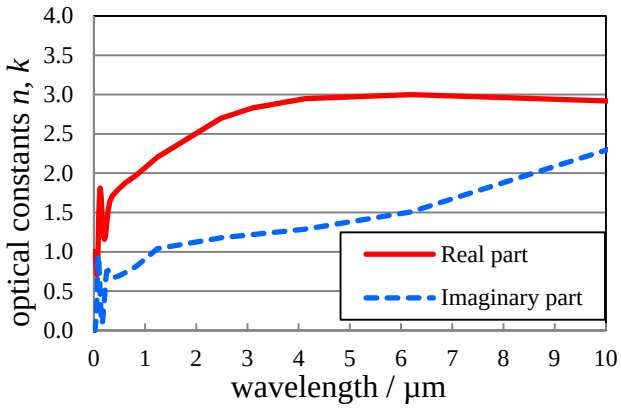

Figure 2: Refractive index of amorphous carbon [20]

Figure 3 shows 2D Finite Difference Time Domain [23] modelled reflectance (*R*) from bulk amorphous carbon and reflectance and transmittance (*T*) for a 35nm thick layer in air. The bulk results show the broadband absorbing properties which are not ideal for reducing thermal infrared emission. The thin film results show the complex optical properties that can occur in thin absorber layers as discussed in our previous paper [24].

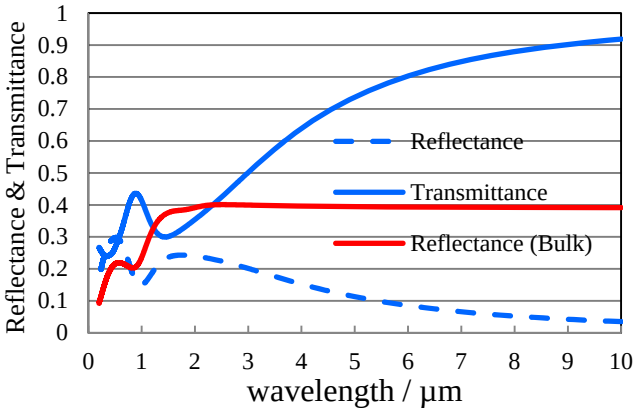

Figure 3: 2D-FDTD simulation of reflectance and transmittance for 35nm and bulk amorphous carbon in air

The absorbance (*A*) can be derived from this data from $T + R + A = 1$. Figure 4 shows absorbance for the bulk case and three layer thicknesses that will be used later in the paper. The results show that thin layers can maintain reasonable absorbance in the visible and this drops off significantly at longer wavelengths. The simplest way of improving the selectivity of such a thin layer is to place it on a strong reflector such as a metal. This approach is used with cermets [25] where the long wavelengths essentially do not “see” the thin layer and strongly reflect from the backside metal.

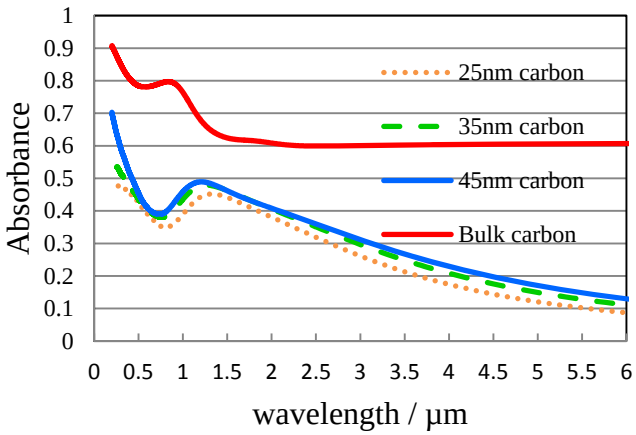

Figure 4: 2D-FDTD simulation of absorbance for various thicknesses of amorphous carbon in air

Figure 5 shows results for a metal backed thin absorbing layer, where the carbon is placed on 200nm of gold. This metal can be used to around 500K [26], [27] and will allow initial room temperature and medium temperature studies to be performed in future. Later in the paper we show results using the high melting point metal tungsten. Gold is straightforward to deposit in cleanroom facilities thus we are focusing the majority of our results on it in these initial studies as others have done [28]. With the Au backing layer, the total absorbance is now significantly different from the simple thin layer case in air. This is due the overlap between the absorbing layer and the standing wave interference pattern generated by the reflecting metal surface. A perfect metal layer imposes a boundary condition of zero tangential electrical field minimising the intensity at the metal surface. At longer infrared wavelengths gold is close to an ideal metal and since the amorphous carbon layer is much thinner than the wavelength this will significantly reduce the absorption in that layer. At visible wavelengths, gold is plasmonic in nature which allows fields to exist within the metal, strongly confined to the surface. Thus, through the boundary conditions between gold and carbon (which are more complex that for simple dielectrics) strong fields will also exist within the carbon layer enhancing the absorption. This absorbance profile is now much closer to the ideal case discussed earlier. However if the absorbance between 1-2µm could be increased without increasing the absorbance at longer wavelengths this would further improve the performance. It can be seen in Figure 5 that increasing the thickness improves absorbance around 2µm, but also at longer wavelengths.

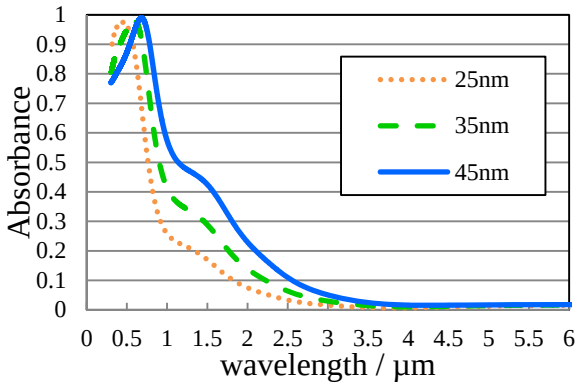

Figure 5: 2D-FDTD simulation of absorbance for various thicknesses of amorphous carbon coated on 200nm Au layer

Thus a more complex structure that allows optimisation of the surface impedance whilst maintaining strong absorption is needed. The MDM structures referred to earlier allow just such optimisation to be performed. MDM structures have been widely studied as absorbers, but mainly with low loss dielectric interlayers where absorption occurs in the metal layers. Here the use of an absorbing interlayer enables the high field strengths generated in the narrow gaps between the upper and lower metal layer to generate very strong absorption. The operating principle of a square array MDM metasurface is now well established [15] and operates by combining an electrical resonance associated with the upper metallic 2D grating and a magnetic resonance generated by gap plasmons between the metal layers. Optimising the period and aspect ratio of the squares allows impedance matching to free space to be achieved which reduces the reflection. This enables strong absorption to occur with appropriate materials either in the metal layers or in our case both in the metal and amorphous carbon layers. Figure 6(a) below shows a 2D schematic of the MDM structure.

In this section of the paper we perform 2D FDTD modelling since this is much faster than 3D modelling and the 2D structure can be made reasonably polarisation independent by creating a 2D grating in the 3D structure as we have shown previously [29]. In order to obtain strong plasmonic interaction with the structure the light must be polarised in the *x* direction as defined in Figure 6(a) and all results in this section are for this case. Figure 6(a) shows the geometrical parameters that can be optimised, the period (*p*), spacing (*s*), length (*l*), thickness (*t*) and height (*h*). The ratio of *l*/*s* is denoted *r*. In order to initiate optimisation of the structure we have chosen 2µm as the design wavelength and we will attempt to maximise the absorption at this wavelength. Figure 6(b) shows a surface plot of period *vs* aspect ratio for a carbon thickness of 35nm. It can be seen that *A* is maximised at a period of 175nm and an aspect ratio of 6:4. This results in *l*=105nm and *s*=70nm. It is necessary to now observe the overall absorption of this structure across the whole wavelength range of interest.

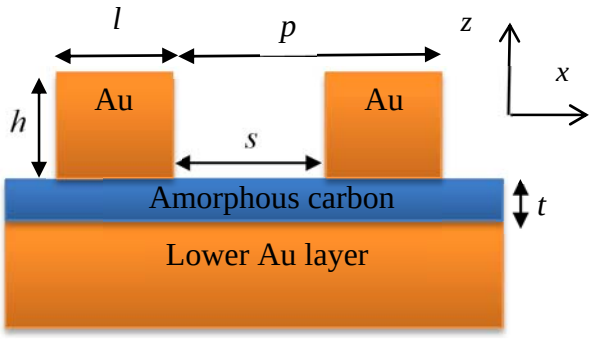

Figure 6(a): Geometrical parameters of the metal-dielectric-metal structure with amorphous carbon as the interlayer. All 2D results below have incident light polarised in the x direction

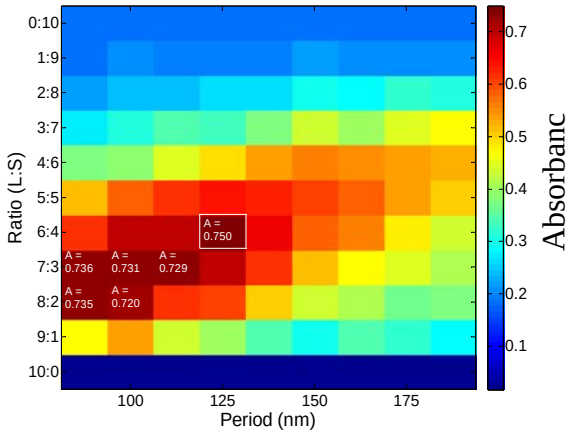

Figure 6(b): 2D-FDTD simulation of absorbance for aspect ratio, r = 0-1, period, p = 100-300nm, carbon thickness, t = 35nm, lower Au thickness = 200nm, wavelength = 2µm

Figure 7 shows absorbance for a range of periods from 150nm to 250nm. The results show that a period of 175nm produces a shoulder that increases the absorption across the 1-2µm range without significantly increasing the absorption at longer wavelengths. A large drop in absorption is observed around 400nm and this will be addressed later in the paper.

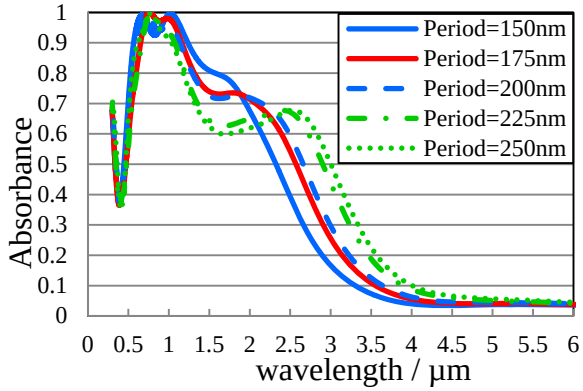

Figure 7: 2D-FDTD simulation of absorbance with x polarization for different periods ranging from 175nm to 250nm with fixed aspect ratio, r = 1.5, carbon thickness, t = 35nm, lower Au thickness= 200nm

Figure 8 summarises the impact of moving to an optimised trilayer structure and shows the significant increase in absorption around 1-2µm. The figure also shows the impact of moving to tungsten for both the upper and low metal layers and it can be seen that good performance is maintained. Finally the figure shows a full 3D simulation of a square array of squares for the top layer, showing that 2D modelling gives a good approximation to the full 3D case. The results give identical absorption for both *x* and *y* polarized light, showing that good polarisation independent performance can be obtained. Ideally the absorbance would decrease more rapidly around 2µm to reduce thermal emission as shown in Figure 1, however there are many applications at lower temperatures where this structure would perform reasonably well.

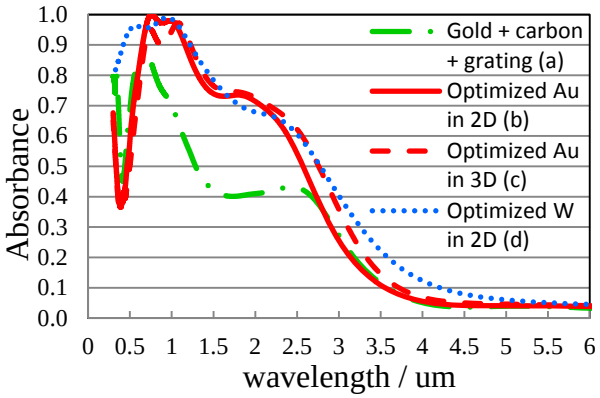

Figure 8: 2D-FDTD simulation of absorbance for the MIM structure start from condition a), Unoptimised gold surface pattern l=150nm, s= 100nm, h=100nm on 35nm amorphous carbon on 200nm gold; b) optimized gold surface patterns l=105nm, s= 70nm, h=100nm; c) same parameters as b) but in 3D simulation; d) same parameters as b) but using tungsten in upper and lower layers

In order to understand the operation of these structures it is useful to observe the electric and magnetic fields in a cross section through the structure at some important wavelengths. Figure 9(a) shows a 3 x 3 section of the structure with cross section A vertically through the centre of grating squares.

Figure 9(b) shows the magnitudes of the electric and magnetic fields in cross section A at wavelengths of 0.4µm, 1.5µm and 5µm. The results show a strong resonance occurring in the magnetic field in the carbon layer at a wavelength of 1.5µm, but much lower field strength at 400nm and 5µm. As noted earlier it is the balance between electric and magnetic resonance that achieves good impedance matching to free space. This strong absorption is caused by an anti-parallel displacement current loops between the upper and lower Au films [30].

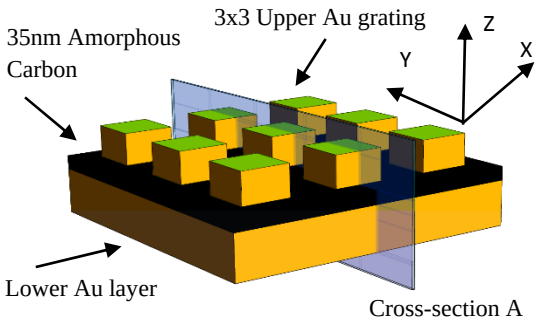

Figure 9(a): Three dimensional schematic view of the MDM showing the cross section plane A

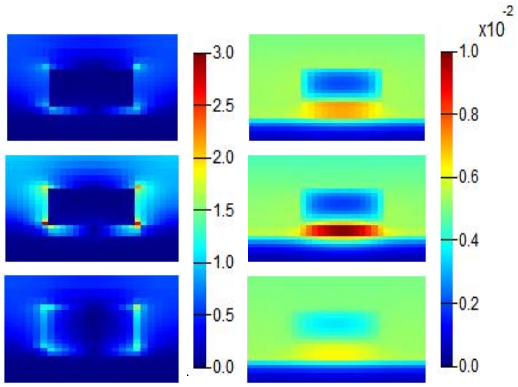

Figure 9(b): Total electric (left) and magnetic (right) field along cross-section A in y-z plane for a single unit cell, carbon thickness= 35nm, l = 105nm, s = 70nm, h = 100nm, wavelength = 0.4µm, 1.5µm and 5µm from top to bottom

Figure 9(b) suggests that the absorption is mainly occurring in the carbon layer but there may also be absorption in the gold layers. We can use the FDTD full field results to directly calculate the absorption in each layer by using the divergence of the Poynting vector as described in our paper [31]. In this approach calculation boxes are placed around each region of interest and this allows the absorption in that region to by calculated directly. Figure 10 shows these results and it can be seen that above 0.5µm the absorption is mainly in the carbon layer.

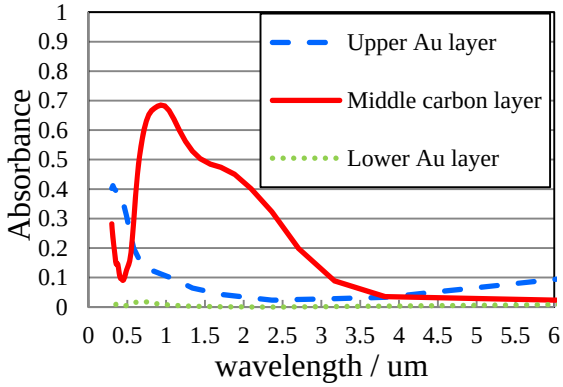

Figure 10: 2D-FDTD simulation of absorbance in each layer for the MIM structure, l=105nm, s= 70nm, h=100nm on 35nm amorphous carbon on 200nm gold

It is important that solar absorbers are as angle independent as possible and one of the main features of the MDM structure is that it is inherently angularly independent. Figure 11 shows reflectance calculated from 0 to 45 degrees over the same wavelength range as shown above. High absorbance (low reflectance) is seen across all angles up to a wavelength of 1.5μm. A low absorption peak (high reflectance) is however visible around 400nm, more clearly visible in Figure 8. In order to improve the absorption here without altering the already optimised longer wavelength range it is necessary to introduce a new degree of freedom into the system.

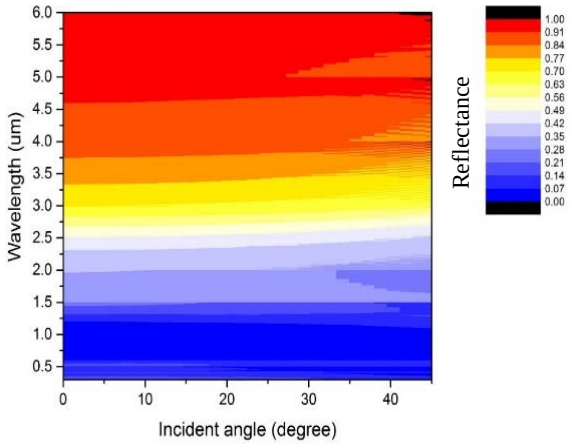

Figure 11: Reflectance of the absorber for surface patterns l=105nm, s= 70nm, h=100nm on 35nm amorphous carbon on 200nm gold for incident light angles from 0 to 45 degree for x polarised light

Figure 12(a) shows such a structure. By moving to a cross based periodic array [17] we are introducing very short arm lengths, *w* that will interact with the shorter wavelengths, with the longer wavelength response being determined by the larger features such as the period and aspect ratio. This gives the extra degree of tunability required to increase the short wavelength absorption. Figure 12(b) shows the performance of a cross structure with different values for *w* compared to the optimised square array case. It can be seen that much stronger absorption can now be obtained around 400nm, but without sacrificing longer wavelength behaviour.

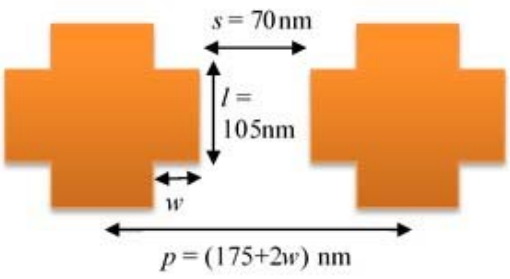

Figure 12(a): Cross type surface pattern with a variable arm length, w

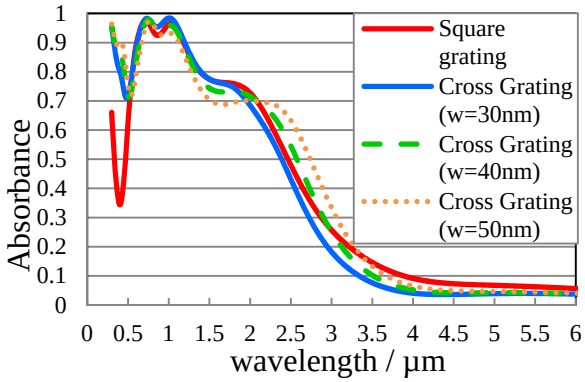

Figure 12(b): 3D-FDTD simulation of absorbance for the grating structures for a simple square array of squares l=105nm, s= 70nm, h=100nm and a square arrays of crosses with variable w, thickness of amorphous carbon = 35nm, lower Au = 200nm

Conclusions

This paper has presented 2D and 3D FDTD modelled results of ultra-thin amorphous carbon films in air, on gold and as the interlayer of a metal-dielectric-metal metasurface for both gold and tungsten. Absorbance results are shown for the structures from wavelengths of 300nm to 6μm. Structure optimisation has been performed in order to achieve good selective surface performance for solar thermal applications. Metal-dielectric-metal metasurfaces based on both square and cross unit cells have been modelled and cross based structure give improved absorption at short visible wavelengths. We believe this is due to the small features within the cross effecting only short wavelength absorption, giving improved solar selectivity. The use of a carbon based inter layer allows us to explore the possibility of using these structures in diamond based solar thermionic applications.

Acknowledgements

The authors would like to acknowledge useful discussion with Dr Sara Nunez-Sanchez, Mr Bofeng Zhu and Dr Neil Fox

Reference:

[1] K. Aydin, V. E. Ferry, R. M. Briggs, and H. A. Atwater, “Broadband polarization-independent resonant light absorption using ultrathin plasmonic super absorbers,” *Nat. Commun.*, vol. 2, p. 517, 2011.

[2] W. Zhou, K. Li, C. Song, P. Hao, M. Chi, M. Yu, and Y. Wu, “Polarization-independent and omnidirectional nearly perfect absorber with ultra-thin 2D subwavelength metal grating in the visible region,” *Opt. Express*, vol. 23, no. 11, p. A413, 2015.

[3] T. Cao, C. Wei, R. E. Simpson, L. Zhang, and M. J. Cryan, “Rapid phase transition of a phase-change metamaterial perfect absorber,” *Opt. Mater. Express*, vol. 3, no. 8, p. 1101, 2013.

[4] Y. Guo, S. Molesky, H. Hu, C. L. Cortes, and Z. Jacob, “Thermal excitation of plasmons for near-field thermophotovoltaics,” *Appl. Phys. Lett.*, vol. 105, no. 7, p. 073903, 2014.

[5] S. Molesky, C. J. Dewalt, and Z. Jacob, “High temperature epsilon-near-zero and epsilon-near-pole metamaterial emitters for thermophotovoltaics.,” *Opt. Express*, vol. 21 Suppl 1, no. January, pp. A96–110, 2013.

[6] E. Rephaeli and S. Fan, “Absorber and emitter for solar thermo-photovoltaic systems to achieve efficiency exceeding the Shockley-Queisser limit.,” *Opt. Express*, vol. 17, no. 17, pp. 15145–15159, 2009.

[7] H. Naito, Y. Kohsaka, D. Cooke, and H. Arashi, “Development of a solar receiver for a high-efficiency thermionic/thermoelectric conversion system,” *Sol. Energy*, vol. 58, no. 4–6, pp. 191–195, 1996.

[8] J. W. Schwede, I. Bargatin, D. C. Riley, B. E. Hardin, S. J. Rosenthal, Y. Sun, F. Schmitt, P. Pianetta, R. T. Howe, Z. X. Shen, and N. A. Melosh, “Photon-enhanced thermionic emission for solar concentrator systems.,” *Nat. Mater.*, vol. 9, no. 9, pp. 762–767, 2010.

[9] K. M. O’Donnell, T. L. Martin, N. A. Fox, and D. Cherns, “The Li-adsorbed C(100)-(1x1):O Diamond Surface,” *MRS Proc.*, vol. 1282, no. 100, pp. 163–168, 2011.

[10] M. Pu, P. Chen, Y. Wang, Z. Zhao, C. Wang, C. Huang, C. Hu, and X. Luo, “Strong enhancement of light absorption and highly directive thermal emission in graphene,” *Opt. Express*, vol. 21, no. 10, pp. 11618–11627, 2013.

[11] J. A. Mason, S. Smith, and D. Wasserman, “Strong absorption and selective thermal emission from a midinfrared metamaterial,” *Appl. Phys. Lett.*, vol. 98, no. 24, pp. 2009–2012, 2011.

[12] C. G. Granqvist, “Spectrally Selective Coatings for Energy Efficiency and Solar Applications,” *Phys. Scr.*, vol. 32, pp. 401–407, 1985.

[13] H. Shin and S. Fan, “All-angle negative refraction for surface plasmon waves using a metal-dielectric-metal structure,” *Phys. Rev. Lett.*, vol. 96, no. 7, pp. 1–4, 2006.

[14] S. Butun and K. Aydin, “Structurally tunable resonant absorption bands in ultrathin broadband plasmonic absorbers,” *Opt. Express*, vol. 22, no. 16, p. 19457, 2014.

[15] J. A. Mason, G. Allen, V. A. Podolskiy, and D. Wasserman, “Strong coupling of molecular and mid-infrared perfect absorber resonances,” *IEEE Photonics Technol. Lett.*, vol. 24, no. 1, pp. 31–33, 2012.

[16] K. Liu, H. Hu, H. Song, X. Zeng, D. Ji, S. Jiang, and Q. Gan, “Wide-angle and polarization-insensitive perfect absorber for organic photovoltaic layers,” *IEEE Photonics Technol. Lett.*, vol. 25, no. 13, pp. 1266–1269, 2013.

[17] Q. Feng, M. Pu, C. Hu, and X. Luo, “Engineering the dispersion of metamaterial surface for broadband infrared absorption,” *Opt. Lett.*, vol. 37, no. 11, p. 2133, 2012.

[18] S. A. Kalogirou, “Solar thermal collectors and applications,” *Progress in Energy and Combustion Science*, vol. 30, no. 3. pp. 231–295, 2004.

[19] J. Robertson, “Diamond-like amorphous carbon,” *Mater. Sci. Eng. R Reports*, vol. 37, no. 4–6, pp. 129–281, 2002.

[20] J. Robertson and E. O’Reilly, “Electronic and atomic structure of amorphous carbon,” *Phys. Rev. B*, vol. 35, no. 6, pp. 2946–2957, 1987.

[21] D. R. Lide and G. Baysinger, “TeamLRN CRC Handbook of Chemistry and Physics,” *ISBN 0-8493-0486-5*, pp. 2–29, 2005.

[22] H. J. Hagemann, W. Gudat, and C. Kunz, “Optical constants from the far infrared to the x-ray region: Mg, Al, Cu, Ag, Au, Bi, C, and A1_2O_3,” *J. Opt. Soc. Am.*, vol. 65, no. 6, p. 742, 1975.

[23] S.T.Chu and S.K.Chaudhuri, “Finite-Difference Time-Domain method for optical waveguide analysis,” *Prog. Electromagn. Res.*, vol. Pier 11, pp. 255–300, 1995.

[24] N. Ahmad, J. Stokes, N. A. Fox, M. Teng, and M. J. Cryan, “Ultra-thin metal films for enhanced solar absorption,” *Nano Energy*, vol. 1, no. 6, pp. 777–782, 2012.

[25] C. N. Tharamani and S. M. Mayanna, “Low-cost black Cu-Ni alloy coatings for solar selective applications,” *Sol. Energy Mater. Sol. Cells*, vol. 91, no. 8, pp. 664–669, 2007.

[26] G. Baffou and R. Quidant, “Thermo-plasmonics: Using metallic nanostructures as nano-sources of heat,” *Laser Photonics Rev.*, vol. 7, no. 2, pp. 171–187, 2013.

[27] N. A. Joy, B. K. Janiszewski, S. Novak, T. W. Johnson, S. H. Oh, A. Raghunathan, J. Hartley, and M. a. Carpenter, “Thermal stability of gold nanorods for high-temperature plasmonic sensing,” *J. Phys. Chem. C*, vol. 117, no. 22, pp. 11718–11724, 2013.

[28] C. Wu, B. Neuner III, J. John, A. Milder, B. Zollars, S. Savoy, and G. Shvets, “Metamaterial-based integrated plasmonic absorber/emitter for solar thermo-photovoltaic systems,” *J. Opt.*, vol. 14, no. 2, p. 024005, 2012.

[29] N. Ahmad, J. Stokes, and M. J. Cryan, “Solar absorbers using 1D and 2D periodic nanostructured nickel films,” *J. Opt.*, vol. 16, no. 12, p. 125003, 2014.

[30] T. Cao, L. Zhang, R. E. Simpson, and M. J. Cryan, “Mid-infrared tunable polarization-independent perfect absorber using a phase-change metamaterial,” *J. Opt. Soc. Am. B-Optical Phys.*, vol. 30, no. 6, pp. 1580–1585, 2013.

[31] C. D. Wang and M. J. Cryan, “Efficiency improvement in organic solar cells with nano-structured ITO electrodes,” *J. Opt.*, vol. 17, no. 6, p. 065901, 2015.